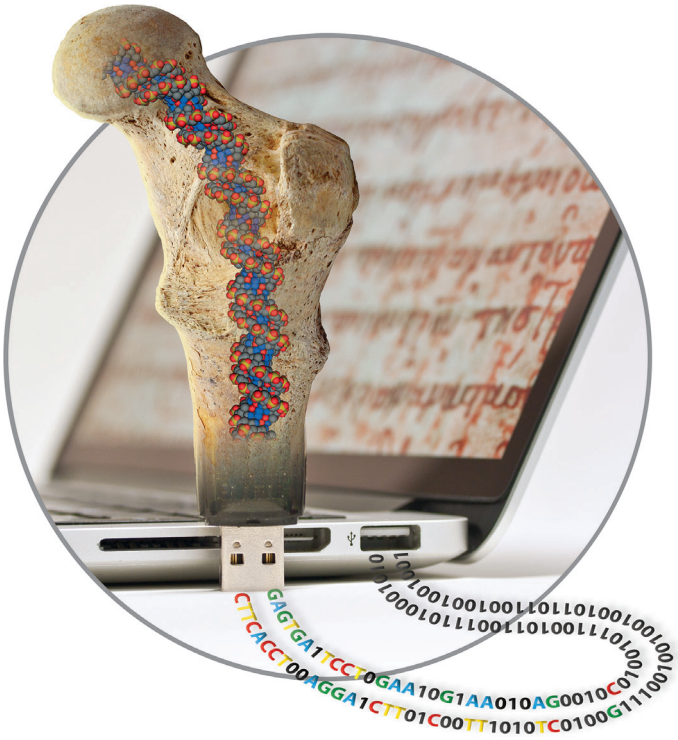

... in our bones may endure for thousands of years, while data written on hard drives will barely survive 50 years. In their Communication on page 2552 ff., R. N. Grass and co-workers show how artificially fossilized DNA (DNA encapsulated in silica) and modern data encoding techniques can be utilized to safely store, for example, the text of the Archimedes Palimpsest for future millennia. The error-correcting codes correct storage-related errors and allow for perfect recovery of the information.

***Hydrogen Oxidation***

In their Communication on page 2340 ff., G. A. Somorjai, J. Y. Park et al. report the effects of Pt nanoparticle size on hot electron flow during hydrogen oxidation. 1.7 nm nanoparticles show a higher catalytic activity than 4.5 nm nanoparticles.

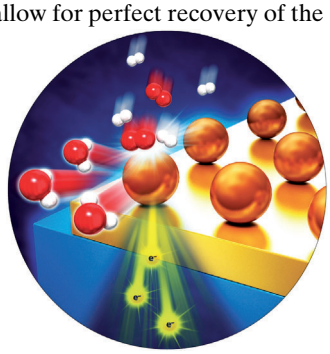

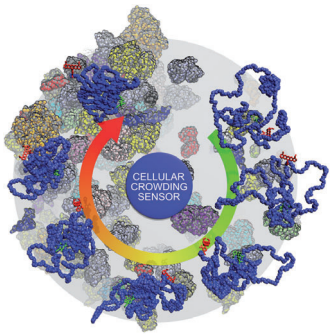


***Macromolecule Biophysics***

S. Ebbinghaus et. al. studied the macromolecular crowding in living cells by using a polymer-based probe. In their Communication on page 2548 ff., they report the effects of osmotic stress on the environment within the cell.

***Supramolecular Chemistry***

In their Communication on page 2457 ff., S. J. Holder, N. A. J. M. Sommerdijk et al. report on the internal morphology of complex polymeric nanospheres and show that the internal structure can be controlled by changing the overall molecular weight and relative hydrophilic content of the composite polymer.

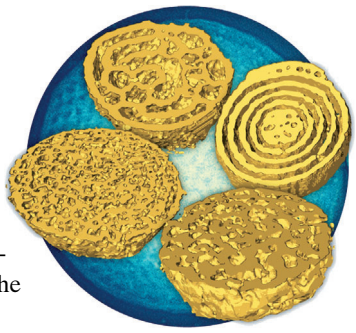

***How to contact us:***

***Editorial Office:***
*E-mail:* angewandte@wiley-vch.de
*Fax:* (+49) 62 01–606-331
*Telephone:* (+49) 62 01–606-315

***Reprints, E-Prints, Posters, Calendars:***
Carmen Leitner
*E-mail:* chem-reprints@wiley-vch.de
*Fax:* (+49) 62 01–606-331
*Telephone:* (+49) 62 01–606-327

***Copyright Permission:***
Bettina Loycke
*E-mail:* rights-and-licences@wiley-vch.de
*Fax:* (+49) 62 01–606-332
*Telephone:* (+49) 62 01–606-280

***Online Open:***
Margitta Schmitt, Carmen Leitner
*E-mail:* angewandte@wiley-vch.de
*Fax:* (+49) 62 01–606-331
*Telephone:* (+49) 62 01–606-315

***Subscriptions:***
www.wileycustomerhelp.com
*Fax:* (+49) 62 01–606-184
*Telephone:* 0800 1800536 (Germany only)
+44(0) 1865476721 (all other countries)

***Advertising:***
Marion Schulz
*E-mail:* mschulz@wiley-vch.de
jspiess@wiley-vch.de
*Fax:* (+49) 62 01–606-550
*Telephone:* (+49) 62 01–606-565

***Courier Services:***
Boschstrasse 12, 69469 Weinheim

***Regular Mail:***
Postfach 101161, 69451 Weinheim

*Angewandte Chemie International Edition* is a journal of the Gesellschaft Deutscher Chemiker (GDCh), the largest chemistry-related scientific society in continental Europe. Information on the various activities and services of the GDCh, for example, cheaper subscription to *Angewandte Chemie International Edition*, as well as applications for membership can be found at **www.gdch.de** or can be requested from GDCh, Postfach 900440, D-60444 Frankfurt am Main, Germany.

GDCh
Gesellschaft Deutscher Chemiker

## Service



## Author Profile



*"If I had one year of paid leave I would work for a Buddhist temple on a mountain whilst studying to become a priest. In a spare hour, I listen to 'new wave' music …"*
This and more about Norio Shibata can be found on page 2318.

## News




A. O'Mullane


B. J. Smith


M. G. Banwell


R. J. Payne


D. M. D'Alessandro


C. Wentrup


G. Gasser


N. Banerji

## Obituaries

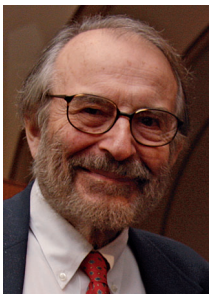



## Books



## Reviews

### Oil/Water Separation



**Stringent segregation**: Superhydrophobic/superoleophilic surfaces and underwater superoleophobic surfaces have been successfully designed, fabricated, and employed in the separation of oil/water-free mixtures and emulsions on the basis of their selective superantiwetting/superwetting properties towards water and oil. Progress, remaining problems, and future challenges in this field are discussed in this Review.

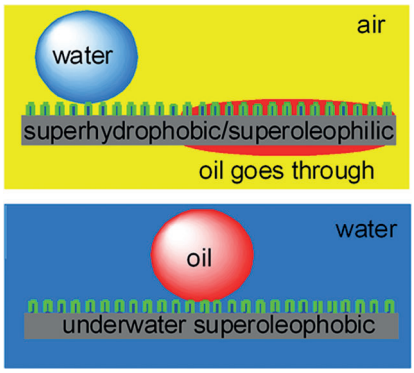


## Communications

### Hydrogen Oxidation



**Catalytic nanodiodes**: Chemically induced hot electron flows on Pt nanoparticles were measured using Au/$TiO_2$ nanodiodes (see picture) and showed the correlation of chemicurrent with catalytic activity. The catalytic nanodiodes with smaller Pt nanoparticles lead to higher chemicurrent, and the temperature dependence is similar to that of the turnover frequency.

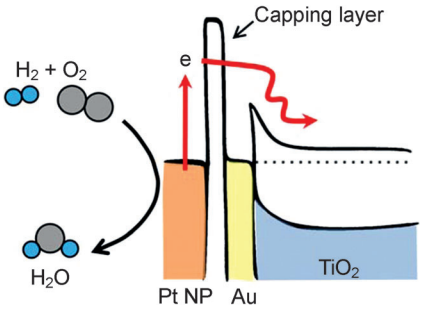




**For the USA and Canada:**
ANGEWANDTE CHEMIE International Edition (ISSN 1433-7851) is published weekly by Wiley-VCH, PO Box 191161, 69451 Weinheim, Germany. US mailing agent: SPP, PO Box 437, Emigsville, PA 17318. Periodicals postage paid at Emigsville, PA. US POSTMASTER: send address changes to *Angewandte Chemie*, John Wiley & Sons Inc., C/O The Sheridan Press, PO Box 465, Hanover, PA 17331. Annual subscription price for institutions: US$ 11.738/10.206 (valid for print and electronic / print or electronic delivery); for individuals who are personal members of a national chemical society prices are available on request. Postage and handling charges included. All prices are subject to local VAT/sales tax.

**Just a pinch**: A small amount of dopant gold nanoparticles (< 5 %) increased the catalytic activity of $\alpha$-$MnO_2$ in water oxidation reactions with the established $[Ru(bpy)_3]^{2+}$–$S_2O_8^{2-}$ system (bpy = 2,2′-bipyridine) by up to 8.2-fold in the photochemical and sixfold in the electrochemical system. The nanoparticle dopant is thought to mediate the electron-transfer steps in the mechanism as shown.

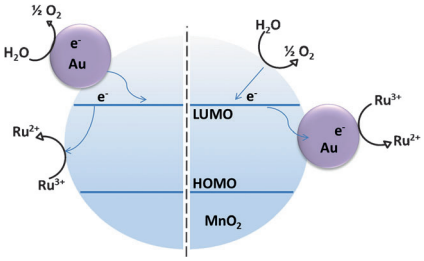


## Water Oxidation Reaction



**A vibrational charge** outside a nanochannel can promote water flux within the channel. A decrease in the distance between the charge and the nanochannel causes an increase in the water net flux, which is contrary to that of the fixed-charge system. This electromanipulating transport phenomenon provides an important new mechanism of water transport confined in nanochannels.

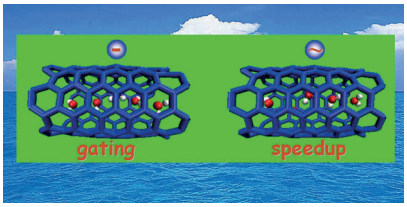


## Nanochannels



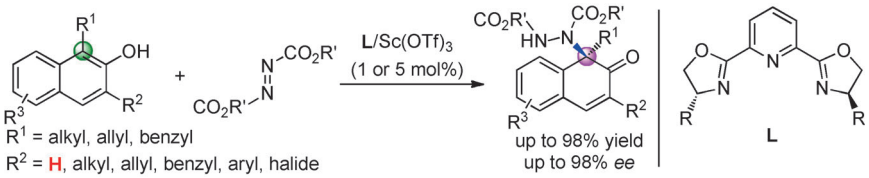


**Asymmetric aminative dearomatization**: The title reaction was successfully implemented with electrophilic azodicarboxylates under the catalysis of chiral $Sc^{III}$/pybox complexes. This reaction represents a hitherto unknown enantioselective C–N bond-forming process through direct dearomatization of phenolic compounds to generate chiral nitrogen-containing quaternary carbon stereocenters. Tf = trifluoromethanesulfonyl.

## Asymmetric Catalysis



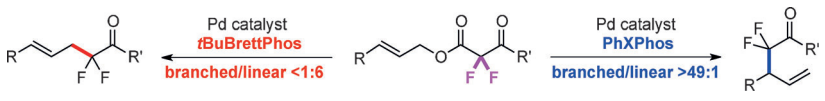


**α,α-Difluoroketones** are useful building blocks for the synthesis of therapeutics and probes for chemical biology. To access this substructure, complementary palladium-catalyzed decarboxylative allylation reactions were developed to provide linear and branched α-allyl-α,α-difluoroketones. The regioselectivity was enabled by the fluorine substituents of the substrate and controlled by the ligand.

## Fluorine

## Black Phosphorus



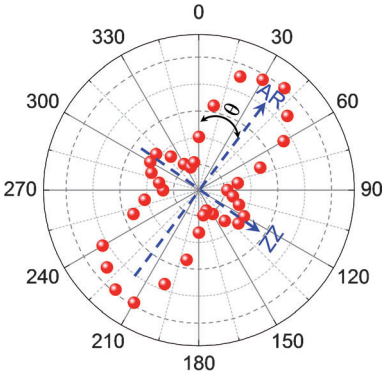


**A compass** to precisely identify the zigzag and armchair directions of black phosphorus (BP) sheets is provided by angle-resolved polarized Raman spectroscopy. The Raman modes of BP show periodic variation (90° or 180°) with the sample rotation angle. Under parallel polarization, the $A_g^2$ mode intensity achieves the larger (or smaller) local maximum when the armchair (or zigzag) direction is along the polarization direction of scattered light.

## Biosynthesis



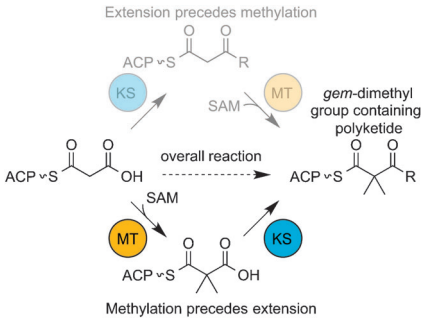


**Order of events**: In order to elucidate the mechanism of *gem*-dimethyl group formation in polyketides, the *gem*-dimethyl group producing polyketide synthase (PKS) modules of yersiniabactin and epothilone were characterized using mass spectrometry. The study demonstrated, contrary to the canonical understanding of reaction order in PKSs, that methylation can precede condensation in PKS modules that produce *gem*-dimethyl groups.

## Synthetic Methods



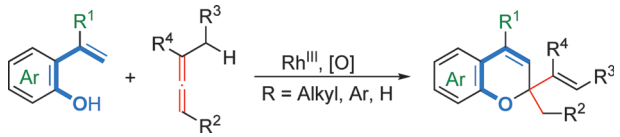


**Skeleton crew**: The synthesis of 2*H*-chromene skeletons was achieved by means of a rhodium(III)-catalyzed oxidative annulation of 2-alkenylphenols and allenes. This unconventional (5+1) process involves the cleavage of the terminal C–H bond of the alkenyl moiety and the participation of the allene as a one-carbon cycloaddition component.

## Natural Product Synthesis



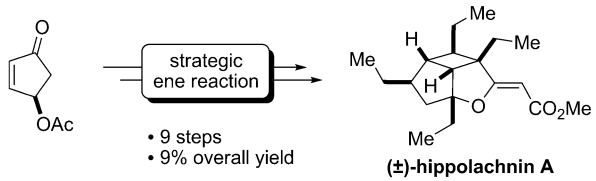


**Brevity makes sweetness!** The first total synthesis of the marine polyketide (±)-hippolachnin A is realized in nine steps and an overall yield of 9%. The synthesis relies on the strategic application of an ene cyclization, which provides rapid access to the oxacyclobutapentalene core skeleton.

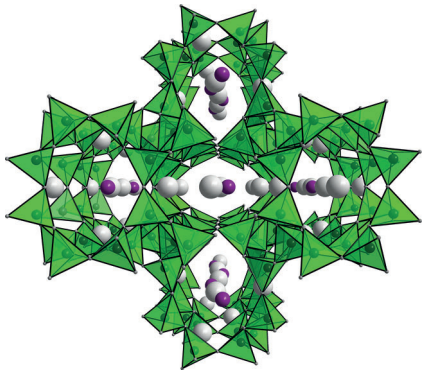

**Under pressure**: A nitridophosphate zeolite $Ba_3P_5N_{10}Br$ was synthesized by a high-pressure/high-temperature reaction at pressures between 1 and 5 GPa and 1000 °C and investigated by single-crystal X-ray diffraction (see picture; Br = purple, Ba = gray, $PN_4$ tetrahedra = green). Doped with $Eu^{2+}$ ions, it exhibits natural-white-light luminescence as a single emitter upon excitation by near-UV light.

## Zeolite Synthesis



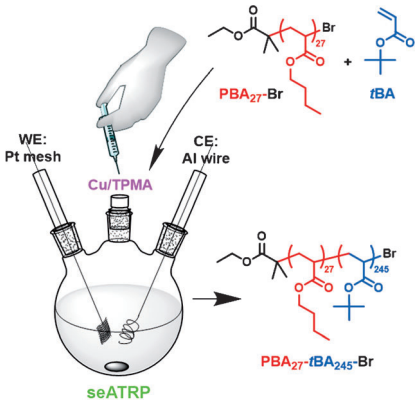


**Take it easy**: Simplification of electrochemically mediated atom transfer radical polymerization was achieved by using an aluminum wire sacrificial anode (*se*ATRP) under potentiostatic or galvanostatic conditions. Homopolymerization and diblock copolymerization show good control of reaction kinetics, providing polymers with molecular-weight evolution close to theoretical values and with narrow molecular-weight distributions.

## Electrochemical Polymerization



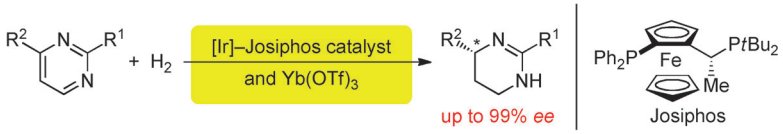


**A chiral catalyst** combining iridium and a lanthanide salt promotes the hydrogenation of pyrimidines to form 1,4,5,6-tetrahydropyrimidines. The reaction of 4-substituted pyrimidines proceeded with high enantioselectivity (up to 99% *ee*) by using a chiral Josiphos ligand (see scheme) for the Ir catalyst.

## Asymmetric Catalysis



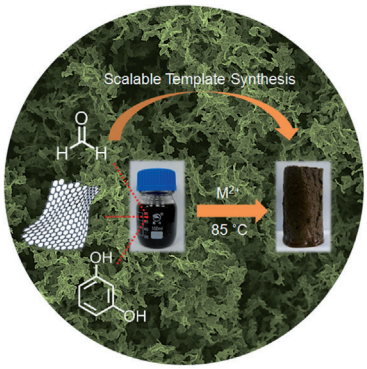


**A composite aerogel** consisting of resorcinol/formaldehyde and graphene oxide (GO) could be synthesized on large scale by using GO sheets as template skeletons and metal ions ($Co^{2+}$, $Ni^{2+}$, or $Ca^{2+}$) as catalysts and linkers. These compressible aerogels can tolerate a strain as high as 80% and quickly recover their original shapes.

## Aerogels

## Stable Organic Radicals



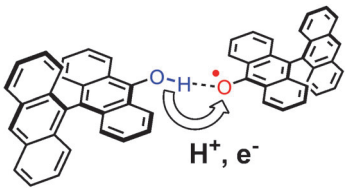


**Self-exchange PCET**: The stable anthroxyl radical was synthesized, and a hydrogen-bonded complex with anthranol was isolated in crystalline form. X-ray analysis at 200 K revealed the activation of the self-exchange proton-coupled electron transfer (PCET) reaction at the hydrogen bond. A strong intermolecular magnetic interaction between radicals causes a phase transition at 125 K that inactivates this reaction.

## Carbon Dioxide Fixation



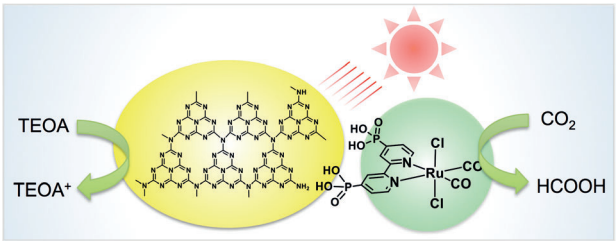


**A heterogeneous photocatalyst** that is based on a carbon nitride material modified by a ruthenium complex enables the reduction of $CO_2$ into formic acid with a high turnover number (>1000) and a good apparent quantum yield (5.7% at 400 nm). These are the highest values that have been reported for $CO_2$ reduction by heterogeneous photocatalysts under visible-light irradiation to date (TEOA = triethanolamine).

## Alkaloids



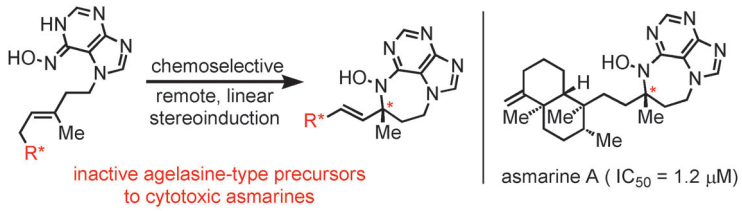


**Unnatural product**: A nitrosopurine ene reaction easily assembles the asmarine pharmacophore and transmits remote stereochemistry to the diazepine-purine heterocycle. This reaction generates potent cytotoxins which exceed the potency of asmarine A and supersede the metabolites as useful leads for biological discovery.

## Dendrimer Synthesis





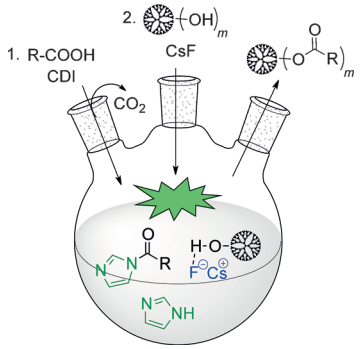


**Esterifications** with 1,1′-carbonyldiimidazole (CDI) were significantly improved by the use of cesium fluoride as the catalyst, which drives these reactions to completion. Structurally flawless and highly functional polyester dendrimers were obtained through a divergent growth approach featuring the fluoride-promoted esterification of hydroxy-functionalized scaffolds with imidazolide-activated monomers.

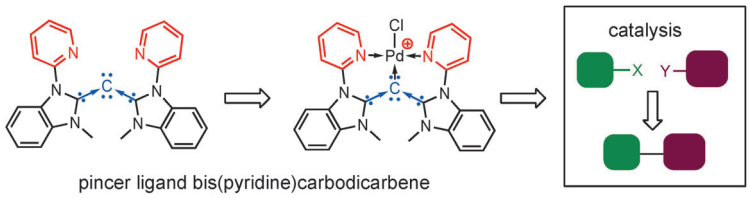


**The acyclic pincer ligand** bis(pyridine)-carbodicarbene was synthesized, isolated, and characterized. It features a C-C-C angle of 143°, which is larger than that in the monodentate framework. Palladium complexes supported by this ligand are active catalysts in Heck–Mizoroki and Suzuki–Miyaura coupling reactions.



**Taking shape**: A $Ru^{3+}$-mediated synthesis has been developed for unique Pd concave nanostructures which can directly harvest UV-to-visible light for styrene hydrogenation (see figure). The catalytic efficiency under full-spectrum irradiation at room temperature turns out to be comparable to that of the thermally (70 °C) driven reaction. The yields are higher than those obtained using Pd nanocrystals such as nanocubes and octahedrons.

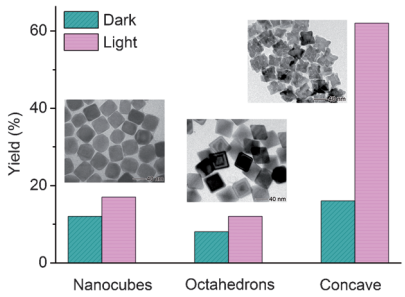




**A novel 3D** gold-DNA superstructure based on DNA growing and origami folding on gold nanoparticles had been fabricated. The new 3D superstructures exhibit great potential for high-efficiency molecule transport for use in cellular imaging and drug delivery.

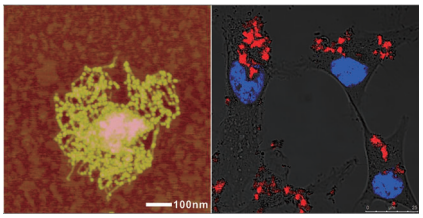




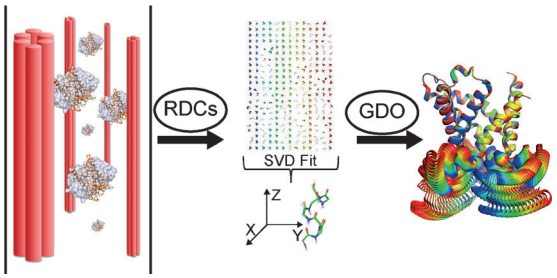


**Flexing domains**: Liquid-state NMR spectroscopy has been used to study conformational heterogeneity of mitochondrial GTP/GDP transporter. The data reveal that the carrier is intrinsically plastic. Despite the threefold pseudo-symmetry of the carrier, the plasticity is asymmetrically distributed among the domains. GDO = generalized degree of order, RDC = residual dipolar coupling.

## Neuron Imaging



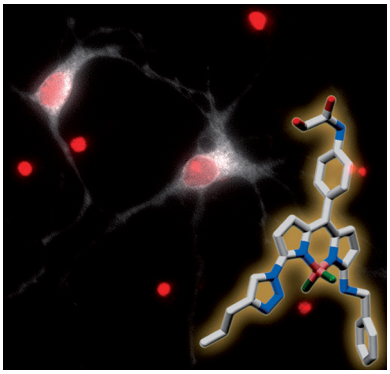

**Selective labeling** of live neurons over other brain cells was achieved with a novel fluorescent probe, **NeuO**. It enables stable, live neuron imaging in vivo and in vitro across species, thus setting the stage for various neuronal targeting applications including the study of neuron development and degeneration.

## G-Quadruplexes



**A transcription check-point**: Transcription through guanine-rich regions produces DNA:RNA hybrid G-quadruplexes. In turn, these regulate transcription by mediating premature termination of transcription.

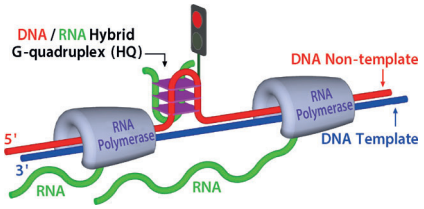


## Nuclear-Spin Polarization



**Hyperpolarization** of molecules utilizing para-hydrogen (red spheres; see picture) and Pt nanoparticles (gray spheres) in water is described. The nanoparticles (diameter ≈ 2 nm) are capped with glutathione ligands (blue lines) to allow for the pairwise addition of para-hydrogen and create observable magnetization. As the solvent is biocompatible, the generation of new molecular imaging contrast agents can be envisioned.

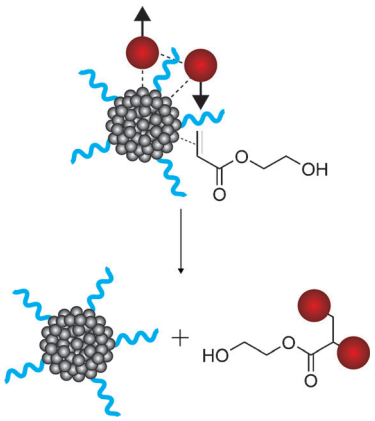


## Supramolecular Chemistry



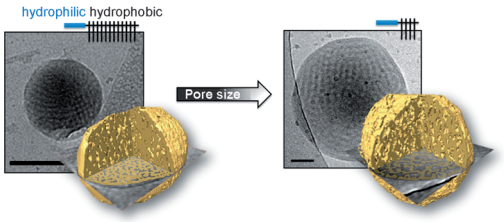


**Tailoring polymer nanospheres**: The relative hydrophilic–hydrophobic content in amphiphilic comb-like block copolymers can be tailored in solution to produce polymeric nanospheres with complex internal morphology. The size and internal pore diameter of the resulting bicontinuous nanospheres can be tuned, showing promise for the formation of nanoporous hybrid materials.

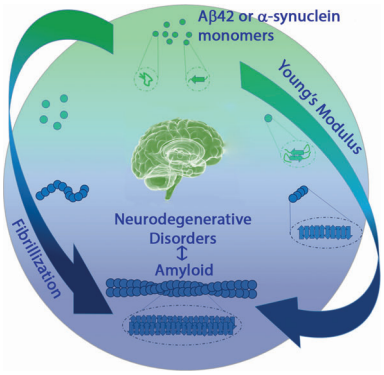


**Inflexibility that comes with age**: During amyloid fibrillization, which is associated with neurodegenerative disorders, initially formed oligomeric and protofibrillar species aggregate to form fibrils with a core cross-β-sheet structure (see picture). AFM peak force quantitative nanomechanical measurements revealed an increase in the Young's modulus during the fibrillization process in conjunction with an increase in the amyloid β-sheet content.

***Biomaterials***



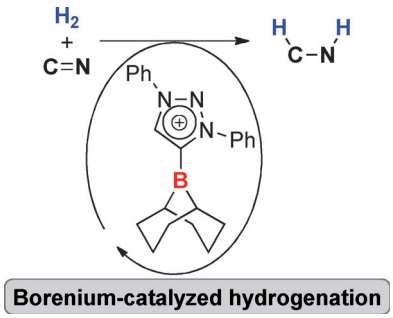


**Size does matter after all**: Tunable, comparatively robust mesoionic borenium ions catalyze the mild hydrogenation of N-containing unsaturated organic functionalities at ambient temperature and ambient pressure. These reactions proceed through a mechanism reminiscent of frustrated Lewis pair chemistry.

***Hydrogenation Reactions***



**The complete transformation** during catalytic operation of crystalline and surface-active $Co_3(PO_4)_2 \cdot 8\,H_2O$ into amorphous and volume-active cobalt oxide reveals basic features of heterogeneous water oxidation catalysis, which is discussed as a convolution of three phenomena: surface catalysis, volume catalysis, and restructuring of the material under operation.

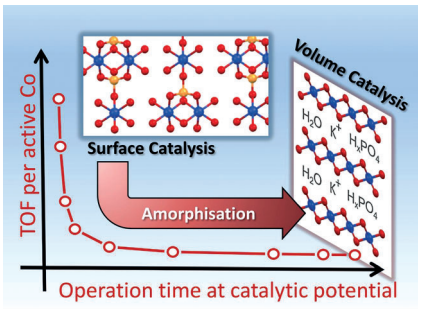


***Heterogeneous Catalysis***



**miRNA profiling:** A versatile hydrogel-based microfluidic approach and novel amplification scheme were used for entirely on-chip, sensitive, and highly specific miRNA detection (let-7a, miR-145, and miR-21; see picture) without the risk of sequence bias. The approach uses photopolymerized hydrogel microposts for miRNA capture and labeling with a universal sequence. Fluorescence products are concentrated into the completely isolated gel posts.

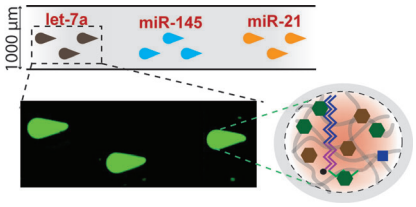


***Diagnostics***

## Cluster Binding



**The backside-ligand** modulation strategy is used to enhance the substrate binding property of Pd clusters. The benzene or naphthalene binding ability of $Pd_3$ or $Pd_4$ clusters is enhanced significantly by the backside cyclooctatetraene ligand (see ovals in scheme), leading to the first isolable $\mu_3$-benzene $Pd_3$ clusters or $\mu_4$-naphthalene $Pd_4$ clusters.

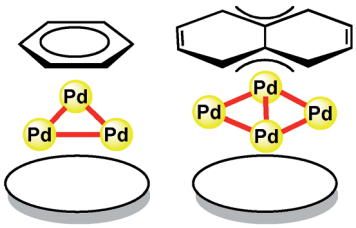


## Radical Cascade Reactions



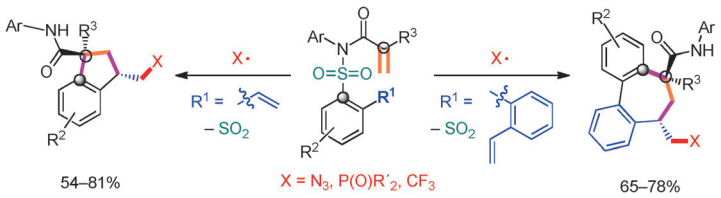


**Densely functionalized** indanes and dibenzocycloheptadienes were produced through highly stereoselective radical-mediated reactions from *ortho*-vinyl- and *ortho*-vinylaryl-substituted *N*-(arylsulfonyl)acrylamides, respectively. The chemoselective addition of in situ generated radicals (X•) onto the styrene moieties initiates a reaction cascade that results in the 5- and 7-membered ring carbocyclic products in a highly efficient manner.

## Biocatalysis



**Best of both worlds**: By fusing a eukaryotic tRNA-recruiting domain (C) to a prokaryotic adenylation domain (A) a new synthetic tRNA-aminoacylation catalyst was created. This catalyst was functionally characterized and was able to load proteinogenic and non-proteinogenic amino acids onto various tRNAs.

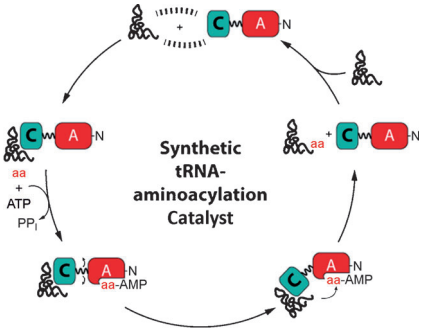


## C–H Amination




**Trimethoxylpyridine** is an efficient ligand for promoting Pd-catalyzed *ortho*-C–H amination of both benzamides and triflyl-protected benzylamines. This finding provides guidance for the development of ligands that can improve or enable $Pd^{II}$-catalyzed $C_{sp^2}$–H activation reactions directed by weakly coordinating functional groups.

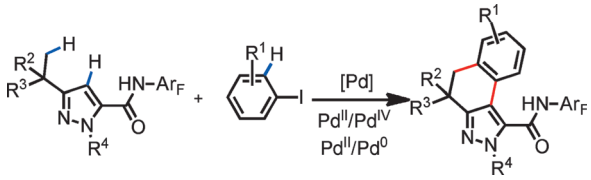


## Cascade C–H Activation



**Benzo[*e*]indazole derivatives** are obtained by a sequential triple C–H activation directed by a pyrazole and an amide group. This cascade reaction demonstrates that the often problematic competing C–H activation pathways in the presence of multiple directing groups can be utilized to improve step economy in synthesis. Pyrazole as a relatively weak coordinating group is shown to direct $C_{sp^3}$–H activation.

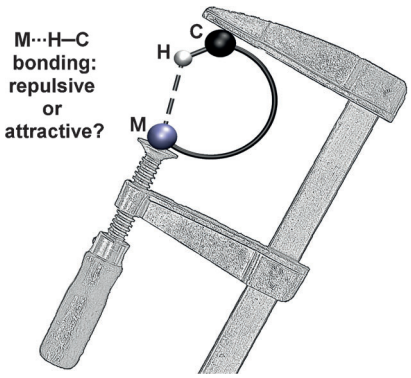


## Agostic Interactions



**Weakly attractive** 3c–2e M···H–C agostic interactions can be established in square-planar $d^8$-$ML_4$ complexes. A new characterization method is used to probe these interactions under pressure by combined high-pressure IR and X-ray diffraction studies. The use of the sign of $^1$H NMR shifts as major criterion to classify M···H–C interactions as attractive (agostic) or repulsive (anagostic) is called into question.

**... and BOB's your uncle**: A fluorescent probe of mitochondrial polarity, termed BOB, showed a linear ratiometric fluorescence response to solution polarity. Various mitochondria of normal cells and cancer cells were examined, and it was found that mitochondrial polarity tends to be lower in cancer cells than in normal cells. The detection of mitochondrial polarity could thus be used as a method to distinguish cancer cells from normal cells.

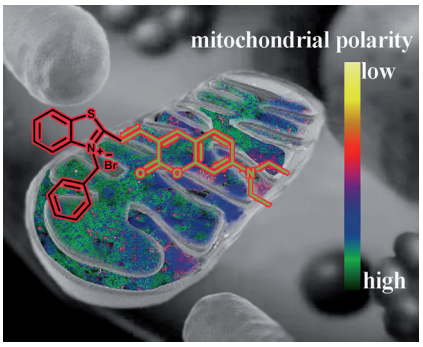


## Cellular Imaging



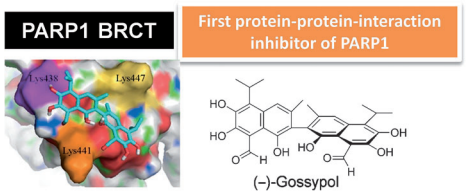


## Protein–Protein Interactions



**Array and break**: By establishing a high-throughput microplate-based assay for screening potential inhibitors of protein–protein interactions of the PARP1 BRCT domain, (–)-gossypol was found to possess novel PARP1 inhibitory activity both in vitro and in cancer cells, presumably by acting as a chemical dimerizer of the PARP1 BRCT domain, which causes disruption of protein–protein interactions and leads to inhibition of the enzymatic activity.

  

## Asymmetric Cyclization



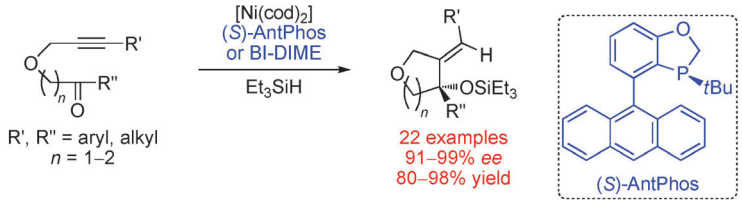


**A P-chiral monophosphine** is used as the ligand in the first asymmetric nickel-catalyzed intramolecular reductive cyclization of alkynones. This transformation enabled the formation of a series of tertiary allylic alcohols bearing furan/pyran rings in excellent yields and enantioselectivities and the efficient synthesis of dehydroxycubebin and the chiral dibenzocyclooctadiene skeleton.

## Nanorobotics



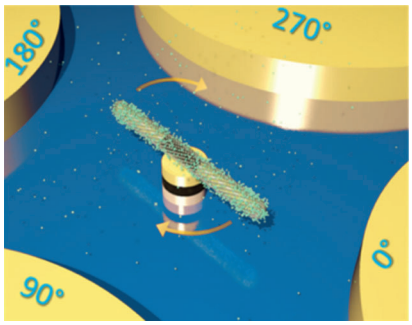


**Motorized nanomotor sensors** are used to tune the release rate of biochemicals and allow their real-time detection. The nanomotor sensors are assembled from designed nanoentities and can be rotated controllably. Both single and multiple biochemicals can be released from the rotating nanomotor sensors in a tunable fashion.

## DNA Nanotechnology



**Logic antibody locks**: Bivalent peptide–DNA conjugates are presented as generic, noncovalent, and easily applicable molecular locks that allow the control of antibody activity using toehold-mediated strand displacement. By connecting antibody-based molecular recognition and DNA-based computing, this new approach allows the introduction of autonomous signal-processing in antibody-based targeting.

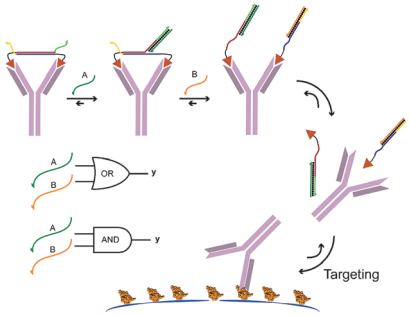


## MOF Phase Transitions



**Multiply the unit cell**: An ammonium Mg formate framework has a rare three-dimensional binodal framework with long cavities accommodating 1,3-propanediammonium and water. The framework displays a phase transition at 275 K to give a 36-fold multiple unit cell and anisotropic switchable dielectric responses.

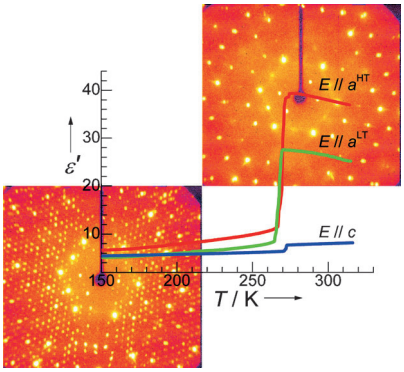

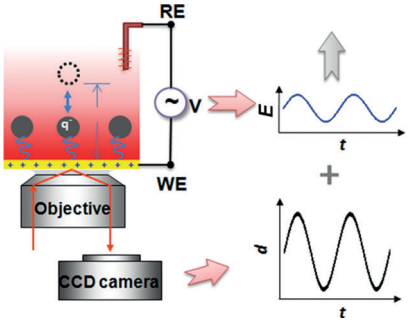


**The phosphorylation kinetics** of a few peptide molecules could be monitored in real time with self-assembled nano-oscillators. Each oscillator consists of a gold nanoparticle tethered to a gold chip with a molecular linker.

## Charge-Based Detection



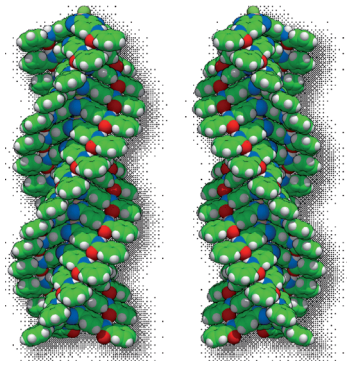

**Piling up** rigid tetrahedral-shaped subphthalocyanine dye molecules in a convex-to-concave fashion results in the formation of unconventional homochiral noncentrosymmetric columnar assemblies (see picture). Assembly occurs through a cooperative supramolecular polymerization process driven by a combination of noncovalent interactions (C green, N blue, O red, H white).

## Supramolecular Chemistry



**Crowding in cells:** A FRET-labeled homopolymer serves as a sensor to study macromolecular crowding in single living cells. Contrary to expectations, the cellular environment does not lead to a compression of the sensor. The sensor is further utilized to probe sub-cellular heterogeneities and crowding changes upon osmotic stress.

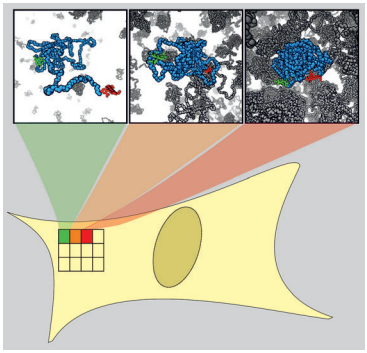

## Macromolecule Biophysics



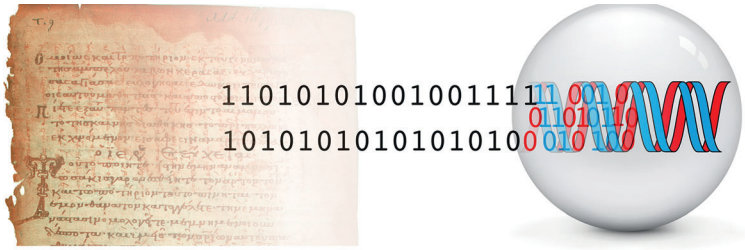


**Committing to memory**: Digital information can endure thousands of years of storage when translated into ACGT nucleotide coding and encapsulated as DNA in silica glass spheres. This method was demonstrated with the digitalized Archimedes Palimpsest.

## Long-Term Memory

## Mechanophores



**Caught in the act:** A 1,4-diaryl-1,2,3-triazole was embedded in a poly(ethylene glycol) chain and additionally bridged by an aliphatic chain. Single polymer molecules were then stretched in an atomic force microscope. Mechanochemical bond rupture in the macrocycle leads to a defined length increase of the polymer of more than 1 nm, which is large enough to be measured directly for a single molecule.

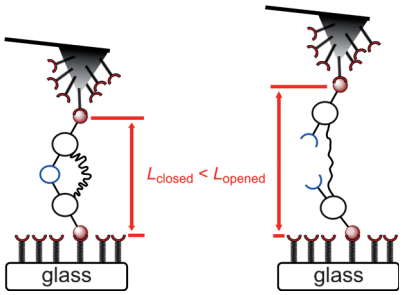


Supporting information is available on www.angewandte.org (see article for access details).

A video clip is available as Supporting Information on www.angewandte.org (see article for access details).

This article is available online free of charge (Open Access).

This article is accompanied by a cover picture (front or back cover, and inside or outside).

The Very Important Papers, marked VIP, have been rated unanimously as very important by the referees.

The Hot Papers are articles that the Editors have chosen on the basis of the referee reports to be of particular importance for an intensely studied area of research.